ELSEVIER

Robotics and Autonomous Systems 13 (1994) 233–243

Robotics and Autonomous Systems

A robot-task conformance index for the design of robotized cells

Guy M. Cloutier [a,*], Alain Jutard [b], Maurice Bétemps [b]

[a] *Dépt. de Génie Industriel, École Polytechnique, C.P. 6079, succ. Centre-Ville, Montréal, Québec, Canada H3C 3A7*
[b] *Laboratoire d'Automatique Industrielle, INSA de Lyon, 69621 Villeurbanne, Cedex, France*

Communicated by T.C. Henderson
Received 1 October 1993; revised 8 April 1994

Abstract

A *robot-task conformance index* is introduced. It applies to any manipulator and a broad scope of tasks. Bounded in the [0, 1] range, this dimensionless index is defined within or outside singularities, and remains invariant against changes in units for translations or rotations. It is based on the simultaneous diagonalization of quadratic forms accounting for the "capabilities" of the robot and the "constraints" of the task. The structural and joint properties of the robot are formulated as a repeatability ellipsoid. A sufficient task ellipsoid is construed from the task's *domain of constraints*. Following the simultaneous diagonalization of both robot and task ellipsoids, *minimum containing* and *maximum contained ellipsoids* are deduced. Appropriate volume ratios of these four ellipsoids define the conformance index. Calculations performed in the diagonalized space reduce the computational burden.

Keywords: Manipulator; Task; Accommodation; (Hyper)ellipsoids; Conformance index

1. Introduction

Many dexterity measures for manipulators were designed. They include the condition number of the Jacobian, the "manipulability" index, the minimum singular value, and others [1–5]. Label these *intrinsic* indices, as they do not relate to the task. The design of dexterous manipulators fostered the conception of these measures [6–9]. The inherent accuracy of such kinematic chains should help the design of better robotic arms. A large pool of industrial robots not so designed nevertheless remain in use. Conventional CAD/CAM tools limit the layout design of robotized cells to a criterion of *reach*. Current robots however suffer from a variable repeatability within their *reachable workspace*. Extrinsic robot-task accommodation indices could bridge the gap between developers and users.

Chiu [10,11] devised (extrinsic) *compatibility* models, weighing *transmission coefficients* of Yoshikawa's (intrinsic) *manipulability ellipsoid* in given "preferred" directions. Lee [12] submitted *suitability* measures, based on the intersection and on the difference of shape between manipulability and "task" ellipsoids. The computation again called for the stipulation of "preferred" directions. How to obtain a meaningful task ellip-

* Corresponding author.

0921-8890/94/$07.00 © 1994 Elsevier Science B.V. All rights reserved
SSDI 0921-8890(94)00008-P

soid, or why prefer some directions remains to be clarified.

These trends beget the question as to the usefulness of intrinsic versus extrinsic indices. Asada [13] showed how the inertial anisotropy of a robot would benefit some tasks. The idea of posture induced compliant robot-task accommodation is found in Bourrières et al. [14]. The study of anisotropic behaviour stirs up ample interest in the design of composite materials. We believe the field of robotics could benefit the same proclivity.

Cloutier et al. [15] restated manipulability ellipsoids to account for joint properties. Expanding their meaning to *repeatability ellipsoids* partially bridged the gap towards the requirements of positionally constrained tasks. Task constraint *subspaces* result in marginal and conditional equiprobability contours of the full repeatability.

An accommodation measure that alleviates the insufficiencies of the reach criterion and respects the anisotropy of a task is warranted. This paper presents an appropriate *conformance index*. The simultaneous diagonalization of a "robot ellipsoid" and a "task ellipsoid" provides the basis of the index. Ground for the model of the robot ellipsoid is found in [15].

The structure of the paper follows. The support for a robot repeatability ellipsoid is summarized. A parallel with a robot compliance ellipsoid is drawn. The construction of a task ellipse is introduced with a planar projection of the "peg in hole" insertion. The concept is enlarged to the five degrees of linkage of a prismatic insertion. The conformance index is developed, and some of its properties presented. The reduction of the computational burden is addressed. Finally, suggestions are made as to the use of the index in the design of robotized cells.

2. Robot ellipsoids

In the tasks to follow, the relevant robot ellipsoids would be those of *equiprobability of pose* and of *compliance*, and their projections and intersections with the constraints subspace of the task. The discussion is mostly abridged to equiprobabilities of pose.

2.1. Equiprobability of pose ellipsoids

The manipulability ellipsoid is given by

$$\boldsymbol{\delta\chi}^{\mathrm{T}}(\boldsymbol{J}\boldsymbol{J}^{\mathrm{T}})^{-1}\boldsymbol{\delta\chi} = 1, \tag{1a}$$

with

$$\boldsymbol{\delta\chi} = \boldsymbol{J}\,\boldsymbol{\delta q}, \tag{1b}$$

where $\boldsymbol{\delta\chi}$ is an $m \times 1$ matrix of small motions ($m \leq 6$) in twistspace, $\boldsymbol{\delta q}$ is an $n \times 1$ matrix of variations in jointspace, and $\boldsymbol{J}$ is the $m \times n$ Jacobian of the robot. The structural properties of the arm alter the jointspace unitary hypersphere $\boldsymbol{\delta q}^{\mathrm{T}}\boldsymbol{\delta q} = 1$ into the twistspace manipulability ellipsoid of Eq. (1a). Manipulability ellipsoids vary with the posture of the arm. Principal directions share a mixed space of small translations and rotations. This creates a theoretical difficulty in the measures of size, eccentricity and orientation. For arms that are mechanically decoupled in jointspace, one of the results of [15] states that equiprobability of pose ellipsoid is given by

$$\wp\left\{\boldsymbol{\delta\chi}\,|\,0 \leq \boldsymbol{\delta\chi}^{\mathrm{T}}\left(\boldsymbol{J}\boldsymbol{\nu}_q\boldsymbol{J}^{\mathrm{T}}\right)^{-1}\boldsymbol{\delta\chi} \leq \kappa\right\}, \tag{2}$$

where

$$\boldsymbol{\nu}_q = \mathrm{diag}\left(\sigma_1^2, \sigma_2^2, \ldots, \sigma_n^2\right), \tag{3}$$

when $\boldsymbol{\delta q}_j \sim N(0, \sigma_j^2)$, $j = 1, \ldots, n$. Equiprobabilities (or *repeatabilies*) would then follow a chi-square distribution with m degrees of freedom. Manipulability and repeatability ellipsoids differ by more than a scale factor: $\boldsymbol{\nu}_q$ seldom is a multiple of the identity matrix, if only because of differences in encoders and gear ratios from joint to joint. With the probabilistic interpretation of repeatability ellipsoids, the sharing of a mixed space of small translations and rotations does not pose the above-mentioned problem. It only indicates one should expect operational space coupling between the two types of error.

2.2. Projections and intersections with a subspace

Let $\boldsymbol{\Phi}$ be a binary selection matrix properly devised for the task. The preproduct by $\boldsymbol{\Phi}^{\mathrm{T}}$ truncates the lines of the Jacobian. This filter relates to the "selection matrix" of hybrid control (see

Whitney [16] for an overview), and serves a similar purpose.

$$\boldsymbol{\Phi} = [\boldsymbol{\varphi}_1 \boldsymbol{\varphi}_2 \cdots \boldsymbol{\varphi}_l], \quad l < m \leq 6, \tag{4}$$

where $\boldsymbol{\varphi}_i$, $i = 1, \ldots, l$ are the components of the orthogonal basis of the subspace pertaining to the task. The following can be proven [17]:

$$\mathit{II}_l \equiv (\boldsymbol{\Phi}^{\mathrm{T}} \boldsymbol{J}\boldsymbol{J}^{\mathrm{T}} \boldsymbol{\Phi})^{-1} = 1 \tag{5}$$

is a manipulability projection defining a velocity envelope in the subspace spanned by the residual lines of the Jacobian;

$$\mathcal{I}_l \equiv \boldsymbol{\Phi}^{\mathrm{T}} (\boldsymbol{J}\boldsymbol{J}^{\mathrm{T}})^{-1} \boldsymbol{\Phi} = 1 \tag{6}$$

is a manipulability intersection with the subspace of $\boldsymbol{\Phi}$, defining a velocity envelope;

$$\mathit{II}_f \equiv \left(\boldsymbol{\Phi}^{\mathrm{T}} (\boldsymbol{J}\boldsymbol{J}^{\mathrm{T}})^{-1} \boldsymbol{\Phi}\right)^{-1} = 1 \tag{7}$$

is a projection of a "force ellipsoid", defining an envelope of efforts in the subspace of $\boldsymbol{\Phi}$;

$$\mathcal{I}_f \equiv \boldsymbol{\Phi}^{\mathrm{T}} \boldsymbol{J}\boldsymbol{J}^{\mathrm{T}} \boldsymbol{\Phi} = 1 \tag{8}$$

is an intersection of a "force ellipsoid" with the subspace spanned by the residual lines of the Jacobian, defining another envelope; adding the variance matrix $\boldsymbol{\nu}_q$, Eq. (5) becomes an expression for the marginal probability density distribution, and Eq. (6) develops into a conditional density distribution. Compliance ellipsoids follow a dual pattern with Eqs. (7)–(8), given the introduction of the joint compliance matrix into the equations.

2.3. Repeatability and compliance ellipsoids

The "force ellipsoid" matrix $\boldsymbol{J}\boldsymbol{J}^{\mathrm{T}}$ is analogous to a compliance ellipsoid matrix

$$\boldsymbol{K} = \boldsymbol{J}\boldsymbol{S}\boldsymbol{J}^{\mathrm{T}}, \tag{9}$$

where $\boldsymbol{S}$ is the joint compliance matrix, often assumed to be diagonal:

$$\boldsymbol{S} = \mathrm{diag}(s_1, s_2, \ldots, s_n). \tag{10}$$

The full Cartesian compliance matrix $\boldsymbol{K}$ links the external efforts $\boldsymbol{F}$ and the differential displacements $\delta\boldsymbol{\chi}$ by

$$\delta\boldsymbol{\chi} = \boldsymbol{K}\boldsymbol{F}. \tag{11}$$

The ideal Cartesian compliance matrix is fully decoupled. When examining the *natural* compliance of a SCARA robot, it is customary to invoke the "natural" subspace of the arm by the introduction of a $\boldsymbol{\Phi}$ filter in

$$\boldsymbol{K}_{\varphi} = \boldsymbol{\Phi}^{\mathrm{T}} \boldsymbol{J}\boldsymbol{S}\boldsymbol{J}^{\mathrm{T}} \boldsymbol{\Phi}, \tag{12}$$

thus only retaining the two lateral translations. The comparison of Eq. (12) and Eq. (8) indicates this to be an intersection of the compliance matrix with a subspace considered to be pertinent.

When adopting such an intersection, one marks *preference* for complementary efforts to be *zero*.

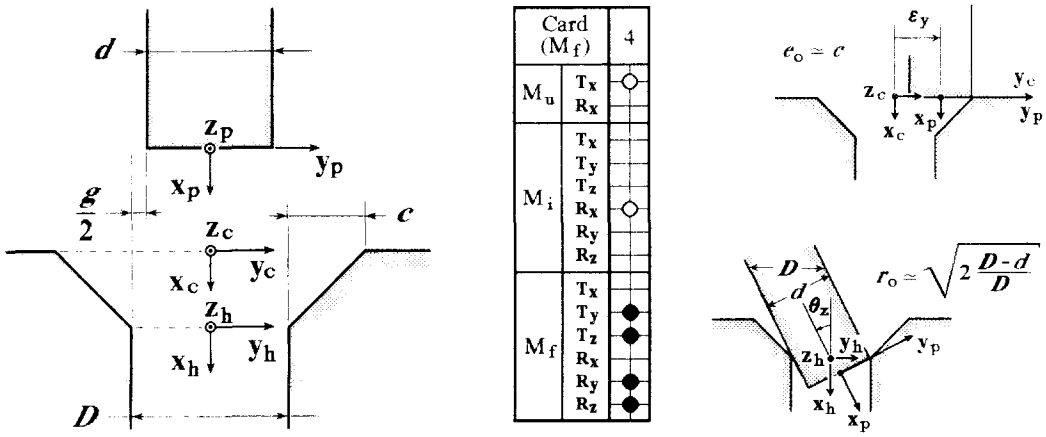

Fig. 1. Planar projection of a "peg in hole" insertion: definition of variables.

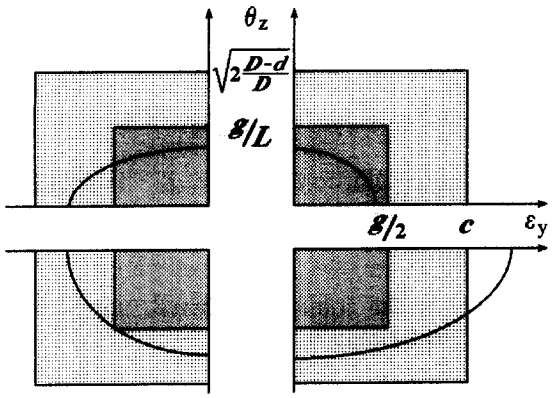

Fig. 2. Planar projection of a "peg in hole" insertion: insertion constraints domains, and four types of repeatability projections in the pertinent subspace.

No (passive or active) feedback will be provided in the complementary subspace. Dually, one concedes *indifference* to the complementary displacements by capitalizing on a marginal probability density distribution governed by $(\Phi^T J v_q J^T \Phi)^{-1}$. They could take *any* value.

3. Task ellipsoid

Robot ellipsoids were interpreted in view of their use with various tasks. The ensuing discussion restricts itself to small displacements. This is by no means a limitation.

3.1. Planar "peg in hole" task ellipse

The macroscopic analysis of the "peg in hole" insertion reveals four forbidden mobilities (M_f), one indifferent mobility (M_i) and one useful mobility (M_u) along the insertion axis. Microscopically, the forbidden mobilities are the ones of interest. Consider a planar projection of this insertion, justified by the axial symmetry of the task. Only two forbidden mobilities then remain along T_y and R_z. This insertion is isotropic in the lateral translations T_y and T_z. It is "anisotropic" in the (T_y, R_z) plane if only because of the dimensional discrepancy of such a plane.

Observe the leeway granted by the task in Fig. 1. With a small gap g, the translation ε_y and rotation θ_z upper-bounds are $e_o \simeq c$ and $r_o \simeq (2(D-d)/D)^{1/2}$ at the onset of the insertion. In first approximation, the e_o and r_o constraints boundaries are decoupled. The ensuing domain is a rectangle centered about the origin, with sides $2e_o$ and $2r_o$. Let L be the depth of the hole. Upon completion of the insertion, the domain is an inner rectangle with sides g along the translation axis and $2g/L$ along the rotation axis.

Fig. 2 displays both domains. It also shows four types of robot repeatability ellipses referenced by quadrant. For a type I repeatability, no ancillary devices or controls are needed. Type II demands translational compliance. Type III commands translational and rotational compliance.

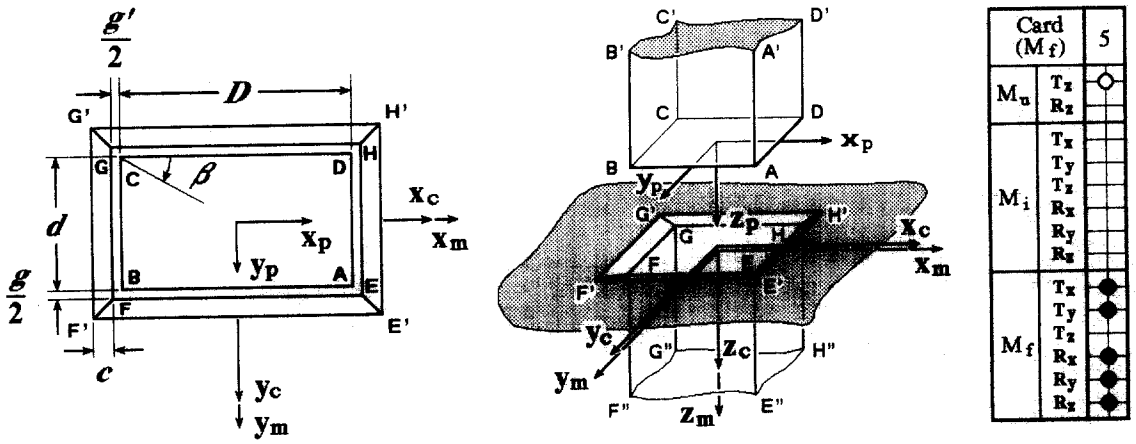

Fig. 3. Prismatic insertion: definition of variables.

Type IV cannot satisfy the onset of the insertion with a good probability. Because the repeatability ellipse of a robot varies with its posture, a single arm might provide types I to IV depending on the layout of the workstation. The goal is to devise a task ellipse (i) that respects the constraints domain, and (ii) that can be used to build a robot-task conformance index.

The proposal is to take the maximum surface ellipse of half-axes e_o and r_o with principal directions confounded with T_y and R_z. The "corners" of the constraints domain are left out of this *sufficient* representation. However, two of the four corners describe a mixed translation-rotation condition detrimental to the insertion. Also, the comparison to come will be made between this sufficient task ellipse and the marginal equiprobability of pose of the arm. There remains a probability that a pose event will lie outside the forecasted repeatability ellipse. Care should be taken when choosing a value for κ in Eq. (2).

3.2. Task ellipsoid for prismatic insertion

The ease with which one derives the constraints domain and the sufficient task ellipse for the preceding insertion is misleading. In most instances, the definition of the domain and its task ellipsoid is by no means trivial.

Take the prismatic insertion of Fig. 3, with five degrees of linkage resulting in five partially coupled constraints. Experiments in passive compliance show the assembly of the prism in the mortise takes place in two (quasi) independent steps: (i) centering, and (ii) reorientation. The centering takes place within the chamfer. The reorientation is accomplished at the top of the mortise. The centering affects variables in T_x, T_y and R_z. The reorientation alters variables in R_x and R_y. Although both steps are independent, the small depth of the chamfer supports the postulate that the adjustments physically take place in the same frame, although not at the same time.

Step (i): Centering

With no R_z misorientation ($\theta_z = 0$), the width c of the chamfer upper-bounds translations ε_x in T_x and ε_y in T_y. The positional constraint is coupled when $\theta_z \neq 0$. The coupling depends on whether corner A or D of the prism reaches the outer limit of the chamfer first. It can be proven [17] that the coupling equations are

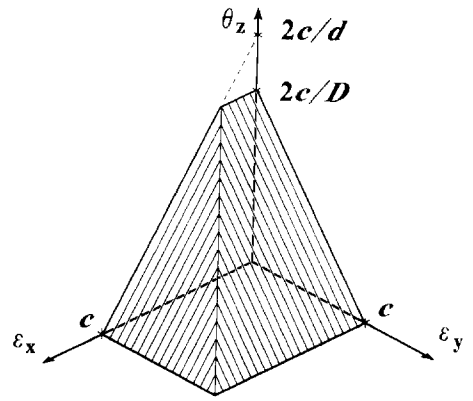

Fig. 4. Prismatic insertion, centering: constraints domain.

$$\theta_z^{\mathrm{A}} = \operatorname{asin}\left(\frac{d + g + 2(c - \varepsilon_y)}{\sqrt{D^2 + d^2}} \right) - \beta. \tag{13}$$

$$\theta_z^{\mathrm{D}} = \beta - \operatorname{acos}\left(\frac{D + g' + 2(c - \varepsilon_x)}{\sqrt{D^2 + d^2}} \right). \tag{14}$$

$$\beta = \operatorname{asin}\left(\frac{d}{\sqrt{D^2 + d^2}} \right). \tag{15}$$

Fig. 4 illustrates the first octant of the symmetrical centering constraints domain. The centering task ellipsoid ξ_c will be of the type

$$\frac{\varepsilon_x^2}{e_{cx}^2} + \frac{\varepsilon_y^2}{e_{cy}^2} + \frac{\theta_z^2}{r_{cz}^2} = 1, \tag{16}$$

where

$$e_{cx}^2 = \frac{2D^2 - d^2 + \sqrt{D^4 + d^4 - D^2 d^2}}{3D^2} c^2. \tag{17}$$

$$e_{cy}^2 = \frac{2d^2 - D^2 + \sqrt{D^4 + d^4 - D^2 d^2}}{3d^2} c^2. \tag{18}$$

$$r_{cz}^2 = \frac{4}{3} \frac{D^2 + d^2 - \sqrt{D^4 + d^4 - D^2 d^2}}{D^2 d^2} c^2. \tag{19}$$

Fig. 5 shows cuts of the centering constraints domain, and of the sufficient task ellipsoid. The solid line illustrates the linear approximation of

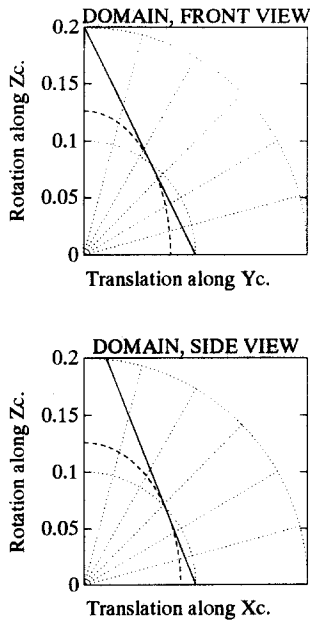

Fig. 5. Prismatic insertion, centering: cut views of constraints domain and task ellipsoids.

the domain when the gaps are negligible. Conditions are: $g = g' = 0.01$ dm; $D = 1.0$ dm; $d = 0.8$ dm; $c = 0.1$ dm.

Step (ii): Reorientation

The maximum misorientation is limited by the edges and the lower corners of the prism, making contact with the side planes and upper edges of the mortise. The contact constraints equations

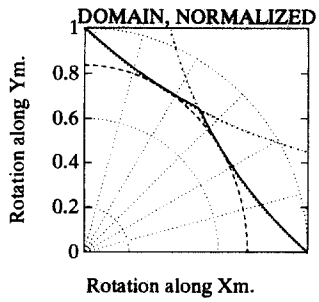

Fig. 6. Prismatic insertion, reorientation: normalized constraints domain and task ellipsoids.

can be developed based on the following sequence (refer to Fig. 3):

- Start with corners D and H superimposed.
- Rotate the prism along its lower edge DC, avoiding the contact between the AA'B'B plane and edge EF.
- Rotate the prism along an axis parallel to y_m, but passing through corner A.
- A point B_o of edge BB' will make contact with the upper edges EF or FG of the mortise, and define the maximum misorientation.

The constraints are found by taking the arc sine of the smallest positive root of

$$\left((D+g')^2 + (d\sin(\theta_x))^2\right)\sin(\theta_y)^2 + 2D(d\sin(\theta_x))\sin(\theta_y) + D^2 - (D+g')^2 = 0. \quad (20)$$

$$\left((D\tan(\theta_x))^2 + (d\cos(\theta_x) - (d+g))^2\right) \times \sin(\theta_y)^2 + 2D(\tan(\theta_x))^2(d\sin(\theta_x))\sin(\theta_y) + (\tan(\theta_x)d\sin(\theta_x))^2 - (d\cos(\theta_x) - (d+g))^2 = 0. \quad (21)$$

Expressing the reorientation in the normalized variable $k_a = (Dg'/dg)^{1/2}$ the square of the half axes of the sufficient (normalized) ellipse $\xi_{o\eta}$ are given by

$$r^2_{o\eta y} = \frac{k_a^4 - k_a^2 - 1 + \sqrt{(k_a^4 - k_a^2 - 1)^2 + 4k_a^6}}{2k_a^4}. \quad (22)$$

$$r^2_{o\eta x} = \frac{1}{k_a^2 r^2_{o\eta y} + 1}. \quad (23)$$

Fig. 6 shows the first quadrant of the normalized constraints domain (solid line), the task ellipse (dashed line), and a local quadratic approximation of the domain (dotted line).

Step (iii): Combined centering and reorientation

Experiments revealed the independence of the centering and the reorientation phases of the insertion. The centering ellipsoid ξ_c thus takes place in a subspace orthogonal to the one of the reorientation ellipse ξ_o. The principal dimensions

of the task hyperellipsoid ξ_t are then simply construed from the previous equations (not normalized), without the introduction of further coupling constraints. This result is a natural consequence of the fact the eigenvectors of an (hyper)ellipsoid are always orthogonal.

4. Robot-task conformance index

Tests and simulations reveal that the robot and the task (hyper)ellipsoids (ξ_r and ξ_t) differ in orientation, eccentricity and volume. No rationale thus supports the adoption of "preferred directions" in their comparison. Instead, a relationship in "all" directions of the constraints subspace seems appropriate [17].

4.1. Overview and rationale

ξ_r and ξ_t contain ellipsoids $\xi_\subseteq$ smaller than their intersection, and are contained in ellipsoids $\xi_\supseteq$ larger than their union. Instead, let $\xi_\subseteq$ designate the largest contained ellipsoid, and $\xi_\supseteq$ be the smallest containing ellipsoid, as in Fig. 7.

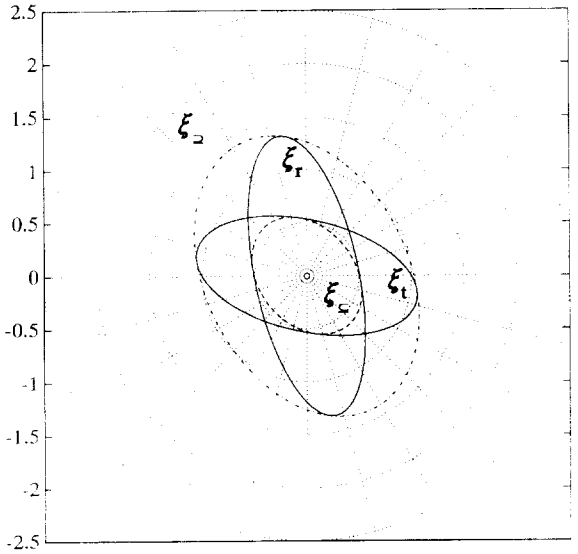

Fig. 7. Basis of conformance index: *robot* (ξ_r), *task* (ξ_t), *largest contained* ($\xi_\subseteq$) and *smallest containing* ($\xi_\supseteq$) ellipsoids.

The *conformance index* is deduced from the "volumes" V_r and V_t of the robot and task ellipsoids, and the volumes $V_\subseteq$ and $V_\supseteq$ of the contained and containing ellipsoids. Clearly, if the ratio $V_t/V_\supseteq = 1$ or the ratio $V_\subseteq/V_r = 1$, then ξ_r is contained in ξ_t. A proper criterion when ξ_r expresses the marginal equiprobability of pose of the robot, and ξ_t reveals the positional constraints of the task. Similar ratios are defined for cases of compliance. The V_t/V_r ratio is generally meaningless. The repeatability might still protrude out of the constraints in some directions, because of differences in shape and orientation.

Properties

(1) Flexible: Provided the robot rests in the jointspace subset that guarantees $V_t/V_\supseteq = 1$ or $V_\subseteq/V_r = 1$, the $V_t/V_r = V_\supseteq/V_\subseteq > 1$ ratio further refines the assessment of the robot-task accommodation. Given that the manipulator rests in the jointspace subset that certifies $V_t/V_\supseteq < 1$ or $V_\subseteq/V_r < 1$, the $V_\supseteq/V_\subseteq > 1$ ratio also complements the conformance index by providing a figure of merit for the "distance" to accommodation.

(2) Dimensionless: The term "volume" is a misnomer when the pertinent subspace shares dimensions in translation and rotation. Task constraints (ξ_t) determine the projection subspace. With this adequate referencing and subspace definition of ξ_r, the proposed ratios will however be dimensionless.

(3) Invariant: The index is invariant against the translational units common to the robot and the task. Units of length usually cause a problem with dexterity indices. The numerical eccentricity of ellipsoids defined in a mixed space of translations and rotations will vary with the units used for translations. The proposed index originates from a ratio taken over the same subspace. It is not affected by a change in translational units, common to both robot and task.

(4) Bounded: Finally, acknowledge the proposed ratios will only vary in the [0, 1] range. An interesting property that helps detect local maxima when the index is used within numerical optimizations.

4.2. Definition of variables

The following are now defined for a context of positional constraints:

- m the number of degrees of linkage of the task, $m = \mathrm{Card}(M_f) \leq 6$;
- α_{tj} the six half axes of ξ_t, only m of which are not infinite;
- Ξ_t the diagonal matrix of eigenvalues $(\lambda_{t1}, \lambda_{t2}, \ldots, \lambda_{t6})$ of ξ_t, only m of which are not zero, $\lambda_{tj} = \alpha_{tj}^{-2}$;
- Ξ_r the 6×6 repeatability matrix of ξ_r, from $(\boldsymbol{J} \boldsymbol{\nu}_q \boldsymbol{J}^T)^{-1}$ (outside singularities);
- $\Xi_{\subseteq}$ the symmetric matrix of $\xi_{\subseteq}$;
- $\Sigma_{\subseteq}$ the diagonal matrix of non zero singular values $(s_{\subseteq 1}, s_{\subseteq 2}, \ldots, s_{\subseteq m})$, from the singular value decomposition (svd) of $\Xi_{\subseteq}$;
- $U_{\subseteq}$ the orthogonal matrix from the svd of $\Xi_{\subseteq}$;

$\Xi_{\supseteq}$, $\Sigma_{\supseteq}$ and $U_{\supseteq}$ are similarly defined for $\xi_{\supseteq}$.

4.3. Basic development

Matrix Ξ_t being diagonal and non negative definite, there exists a unique *square root* matrix $\Xi_t^{1/2}$, such that $\Xi_t^{1/2}\Xi_t^{1/2} = \Xi_t$. From the unicity of the Moore-Penrose inverse, there exists a unique *inverse square root* matrix $\Xi_t^{-1/2}$, such that $(\Xi_t^{-1/2}\Xi_t^{-1/2})^+ = \Xi_t$. A 6×6 projection mask $\boldsymbol{\Phi}$ is then given by

$$\boldsymbol{\Phi} = \left(\Xi_t^{-1/2}\right)^T \Xi_t \Xi_t^{-1/2} \tag{24}$$

Outside singularities, the marginal equiprobability of pose matrix $\Xi_{r\varphi}$ of the robot stems from

$$\Xi_{r\varphi} = \left(\boldsymbol{\Phi} \Xi_r^{-1} \boldsymbol{\Phi}\right)^+, \tag{25}$$

and

$$\Xi'_{r\varphi}\left(\Xi_t^{-1/2}\right)^T \Xi_{t\varphi} \Xi_t^{-1/2}. \tag{26}$$

By the singular value decomposition,

$$\Xi'_{r\varphi} = \boldsymbol{U}_{r\varphi} \boldsymbol{\Sigma}_{r\varphi} \boldsymbol{U}_{r\varphi}^T. \tag{27}$$

The simultaneous diagonalization matrix $\boldsymbol{D}_S$ is

$$\boldsymbol{D}_S = \Xi_t^{-1/2} \boldsymbol{U}_{r\varphi} \tag{28}$$

Matrices $\Sigma_{\subseteq}$ and $\Sigma_{\supseteq}$ are formed from the element by element comparison of the diagonals of $\boldsymbol{\Phi}$ and $\Sigma_{r\varphi}$, taking either the largest or smallest positive values (see Fig. 8).

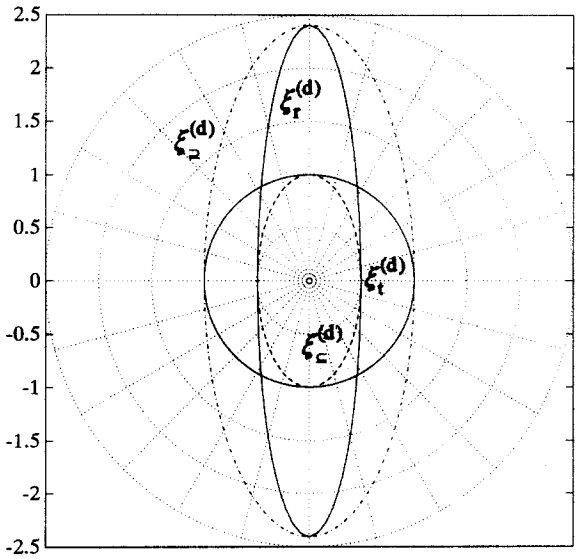

Fig. 8. Basis of conformance index, diagonalized space: same variables as before, with superscript (d).

4.4. Procedural enhancements

For simplicity, the above development was performed with a diagonal task matrix and a robot outside singularities. These are not limitations on the conformance index. If not diagonal, the task matrix will be symmetric. The simultaneous diagonalization then requires a first singular value decomposition of the task matrix. The diagonalization matrix $\boldsymbol{D}_S$ is modified accordingly.

Within singularities, the robot repeatability ellipsoid collapses onto a lower range space. The lost Cartesian mobility results in a null half axis. If the lost mobility lies outside the pertinent subspace of the constraints, the number of finite eigenvalues of the marginal equiprobability remains the same. The diagonalization proceeds as before. If the lost mobility causes the collapse of the marginal equiprobability, an eigenvalue grows to infinity. The infinite eigenvalue generates the null half axis. Because the decomposition performs in the range space, the eigenvalue is numerically forced to zero. This induces the misconception that one of the half axes has grown to

infinity. Though troublesome in control algorithms, singularities benefit the relative positional constraints. A collapsed repeatability means infinite precision. The objective is then to compare the robot and task ellipsoids in a residual pertinent subspace. A solution is to take the projected repeatability of the robot as the new pivot for the diagonalization.

4.5. Reduction of the computational burden

The conformance index C_I was defined as either $V_t/V_{\supseteq}$ or $V_{\subseteq}/V_r$. The volume of an ellipsoid is proportional to the product of its half axes. C_I being a ratio taken over the same subspace, the two proportionality constants are equal and cancel one another.

The simultaneous diagonalization modifies orientations and scale factors. It affects the values of volumes. Conceptually, C_I was defined in the original (non diagonalized) space. Since the conformance index is produced by a *ratio* of volumes, and because the diagonalization transformation is applied to *all* matrices, the ratios of volumes are preserved in the diagonalized space. Consequently, there is no need to transform $\boldsymbol{\Sigma}_{\subseteq}$ and $\boldsymbol{\Sigma}_{\supseteq}$ back to $\boldsymbol{\Xi}_{\subseteq}$ and $\boldsymbol{\Xi}_{\supseteq}$ to calculate the index. Letting the superscript (d) indicate results in the diagonalized space, $C_I^{(d)} = C_I$.

Ellipsoid half axes are equal to the reciprocals of the square roots of eigenvalues. In the diagonalized space, one can calculate a "task referenced" conformance index $C_{It}^{(d)}$

$$C_{It}^{(d)} = \frac{V_t^{(d)}}{V_{\supseteq}^{(d)}} = \frac{\prod_{j=1}^{m} \frac{1}{\sqrt{\lambda_{tj}^{(d)}}}}{\prod_{j=1}^{m} \frac{1}{\sqrt{\lambda_{\supseteq j}^{(d)}}}}, \tag{29}$$

or a "robot referenced" index $C_{Ir}^{(d)}$

$$C_{Ir}^{(d)} = \frac{V_{\subseteq}^{(d)}}{V_r^{(d)}} = \frac{\prod_{j=1}^{m} \frac{1}{\sqrt{\lambda_{\subseteq j}^{(d)}}}}{\prod_{j=1}^{m} \frac{1}{\sqrt{\lambda_{rj}^{(d)}}}}. \tag{30}$$

The task usually being the pivot of the diagonalization, Eq. (29) reduces to

$$C_{It}^{(d)} = \frac{1}{\prod_{j=1}^{m} \frac{1}{\sqrt{\lambda_{\supseteq j}^{(d)}}}} = \sqrt{\prod_{j=1}^{m} \lambda_{\supseteq j}^{(d)}} \tag{31}$$

for greater computational efficiency.

5. Design of robotized cells

The purpose of robotic CAD/CAM tools is to assist the designer in the detailed and global decisions regarding the workstation to come. Alas, commercial CAD/CAM tools limit the layout design of robotized cells to a criterion of *reach*, and the procedures available work best when the cell can be configured *around* the robot. For the designer, the robot is only one of many *tools* to meet the *goal*. The goal is to accomplish the task adequately. From that perspective, the task constraints should constitute the basis for the layout.

Task constraints are both absolute and relative. A criterion of reach responds adequately to the absolute constraints of the task. Relative constraints encompass task tolerances. A suitable conformance index was presented to that effect. How to utterly utilize such an index within the workstation design process remains to be fully developed. Avenues have nonetheless been explored [18,19].

First comes to mind the possibility of superimposing a mesh over the space of the workstation. One of the mesh cells encloses the task. The base of the robot sequentially shifts from cell to cell. Each mesh cell can then be qualified (i) against the reach criterion, and (ii) by the value of the conformance index. Two sets are made available to the designer: the binary *reach set*, and its *conforming subset*. More so, thanks to the bounded range of the conforming index, the conforming subset can be treated as a binary or a continuous variable subset. In the continuous variable subset approach, the designer could analyze tradeoffs in terms of the probability of successful insertion, an obvious benefit.

The prospect to exploit the conformance index in a classical optimization algorithm comes next. The numerical computation of the gradient of the index allows for its use to modify the configuration of the robot using the null space of the Jacobian, while maintaining the absolute position of the tool. Besides, mounting the robot on a mathematical vehicle, optimizations of the conformance index performed in the ensuing null space display absolute positioning of the base of the robot and relative positioning of the links of the arm to accommodate the task constraints better.

Current advances are still being pursued with both approaches.

An apparent flaw of the proposed index comes from considerations underlying the task ellipsoid. One might argue that insertion constraints go beyond the geometrical aspects of the parts. Sturges [20], for one, has modeled the effects of wedging and jamming of the parts. There is no need to limit the analysis leading to the specification of a task ellipsoid to geometrical factors. A sufficient ellipsoid could be lodged in a constraints domain deduced from other physical aspects, provided they are modeled.

6. Conclusion

A *robot-task conformance index* applicable to any manipulator and a broad scope of tasks was introduced. Conceptually wise, this index is not an intrinsic dexterity measure. It rather hinges on what could be called extrinsic *robot-task accommodation* gauging. In so doing, it confronts two implicit assumptions of current commercialized CAD/CAM tools, and potentially provides additional assistance to the designer of a robotized cell.

This index is defined as a proper volumetric ratio founded on (i) the marginal repeatability or conditional compliance of the robot, (ii) the sufficient ellipsoidal constraints of the task, together with (iii) "containing" and "contained" ellipsoids. The specification of *containing* and *contained* ellipsoids follow a simultaneous diagonalization, performed on quadratic forms accounting for the "capabilities" of the robot and the "constraints" of the tasks. Bounded in the [0, 1] range, the dimensionless index remains defined in or outside singularities. It is also invariant against any changes in the units applied for translations and rotations. Calculations performed in the diagonalized space reduce the computational burden.

The index can govern a discrete search over a meshed space, or an optimization algorithm exploiting the null space of the Jacobian. In so doing, this accommodation measure will alleviate the insufficiencies of the reach criterion, and the cell layout will respect the anisotropy of the task.

References

[1] J.K. Salisbury and J.J. Craig, Articulated hands: Force control and kinematic issues, *The International Journal of Robotics Research* 1 (1) (1982) 4–17.

[2] T. Yoshikawa, Manipulability of robotic mechanisms, *The International Journal of Robotics Research* 4 (2) (1985) 3–9.

[3] C.A. Klein and B.E. Blaho, Dexterity measures for the design and control of kinematically redundant manipulators, *The International Journal of Robotics Research* 6 (2) (1987) 72–83.

[4] C. Gosselin and J. Angeles, A global performance index for the kinematic optimization of robotic manipulators, *ASME Intl. Journal of Mechanical Design* 113 (3) (1991) 220–226.

[5] C.M. Gosselin, The optimum design of robotic manipulators using dexterity indices, *Robotics and Autonomous Systems* 9 (4) (1992) 213–226.

[6] J. Angeles and A.A. Rojas, Manipulator inverse kinematics via condition number minimization and continuation, *The International Journal of Robotics and Automation* 2 (2) (1987) 61–69.

[7] J. Angeles and C.S. López-Cajún, The dexterity index of serial-type robotic manipulators, *Proc. 20th ASME Mechanisms Conference*, Kissimme, FL (1988) 74–84.

[8] C. Gosselin and J. Angeles, The optimum kinematic design of a planar three-degree-of-freedom parallel manipulator, *ASME Journal of Mechanisms, Transmissions, and Automation in Design* 110 (1) (1988) 35–41.

[9] C. Gosselin and J. Angeles, The optimum kinematic design of a spherical three-degree-of-freedom parallel manipulator, *ASME Journal of Mechanisms, Transmissions, and Automation in Design* 111 (2) (1989) 202–207.

[10] S.L. Chiu, Control of redundant manipulators for task compatibility, *Proc. 1987 IEEE International Conference*

on Robotics and Automation, Raleigh, NC (1987) 1718–1724.

[11] S.L. Chiu, Task compatibility of manipulator postures, *The International Journal of Robotics Research* 7 (5) (1988) 13–21.

[12] S. Lee, Dual redundant arm configuration optimization with task-oriented dual arm manipulability, *IEEE Transactions on Robotics and Automation* RA-5 (1) (1989) 78–97.

[13] H. Asada and K. Ogawa, On the dynamic analysis of a manipulator and its end effector interaction with the environment, *Proc. 1987 IEEE International Conference on Robotics and Automation*, Raleigh, NC (1987) 751–756.

[14] J.P. Bourrières, P. Jeannier and F. Lhote, Intrinsic compliance of position-controlled robots: Applications in assembly, *Proc. 5th International Conference on Assembly Automation*, Paris (1984) 133–142.

[15] G.M. Cloutier, M. Bétemps and A. Jutard, Workspace design, robotized cells and accommodation of tasks constraints: Basis of a unified approach, *Proc. 8th International Conference on CARS/FOF*, Metz (1992) 1426–1439.

[16] D.E. Whitney, Historical perspective and state of the art in robot force control, *The International Journal of Robotics Research* 6 (1) (1987) 3–14.

[17] G.M. Cloutier, Contribution à l'adaptation robot-tâche; prise en compte et exploitation de l'anisotropie du robot et de l'objet de la tâche en vue de la conception du poste de travail, Thèse de doctorat, Laboratoire d'Automatique Industrielle, Institut National des Sciences Appliquées de Lyon, France (1991).

[18] G.M. Cloutier, C. St-Arneault and L. Cléroux, Robotization of predetermined environments: Solutions to the workstation design problem, *Proc. 8th International Conference on CARS/FOF*, Metz (1992) 1411–1424.

[19] C. St-Arneault and G.M. Cloutier, Workstation design of robotized cells within constrained environments, *Proc. Ind. Automation Conf. and Exhibition*, Montréal, Qc, (1992) 15.13–15.18.

[20] R.H. Sturges, Jr., A three-dimensional assembly task quantification with application to machine dexterity, *The International Journal of Robotics Research* 7 (4) (1988) 34–78.

Guy M. Cloutier received the B.Eng. degree in Electrical Engineering from Ecole Polytechnique, Québec, Canada in 1974, and the degree of "docteur" from the INSA of Lyon, France, in 1991. From 1974 to 1985, he worked in the field of semiconductors, and contributed to the launching of three manufacturing plants. From 1986 to 1991, he was a Research Associate, and since 1992, has been an Associate Professor in the Department of Industrial Engineering, Ecole Polytechnique de Montréal. In 1990 he received the Award for Research Associates from the director of Ecole Polytechnique. In 1993, his research was honored with the French National Award for Thesis on Automation. His research interests emphasize the decision support towards the design of robotized workstations.

Alain Jutard has been Professor in Automation at the "Institut National des Sciences Appliquées" (INSA) de Lyon, France, since 1961. He received the B.Eng. degree in Electronics in 1961, the "docteur-ingénieur" in 1964, and the degree of "docteur d'état en sciences physiques" in 1975. His research interests have covered the field of robotics since 1980. Director of the "Laboratoire d'Automatique Industrielle" (LAI) of Lyon, he has fostered the foundation of the "Atelier Interétablissement de Productique Rhône-Alpes Ouest", and was its first director from 1986 to 1991. He is currently responsible for the doctoral studies in industrial automation at Lyon–Annecy.

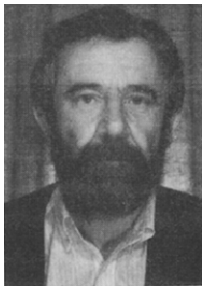

Maurice Bétemps has been Professor in Automation at the "Institut National des Sciences Appliquées" (INSA) de Lyon, France, since 1966. From 1982 to 1986, he contributed to the establishment of the Electro-Mechanical Engineering Department at the engineering school of Sfax, in Tunisia. He is currently responsible for the "Section de Robotique Industrielle" at the INSA of Lyon. He received the B.Eng. degrees in Mechanics and Automation in 1965 and 1966, respectively, and the degree of "docteur d'état en sciences physiques" in 1980. His research interests have covered the field of robotics since 1980.